

## Donor transition energy in GaAs superlattices in a magnetic field along the growth axis

J. M. Shi, F. M. Peeters, G. Q. Hai, and J. T. Devreese\*

*Department of Physics, University of Antwerp (UIA), Universiteitsplein 1, B-2610 Antwerpen, Belgium*

(Received 21 March 1991)

The transition energies between the ground state ( $1s$ -like) and two excited states ( $2p^\pm$ -like) are calculated for shallow donor impurities in GaAs superlattices in the presence of a magnetic field along the growth axis. Results are obtained as a function of the magnetic field and the well width for various widths and heights of the barriers of the superlattices. The dependence of the transition energies on the position of the donors and the effect of band nonparabolicity are also investigated. The calculation is based on a variational approach in which Gaussian-type trial wave functions with two variational parameters are used. Polaron correction to these energies is studied within second-order perturbation theory in which only the three-dimensional-bulk phonon modes of GaAs are included. We found that the polaron effect and band nonparabolicity have to be included in order to correctly describe the experimental transition energies.

### I. INTRODUCTION

With the advances in crystal-growth techniques such as molecular-beam epitaxy and metal-organic chemical vapor deposition, it has become possible to grow systems of alternating layers of two different lattice-matched semiconductors having controlled thicknesses and sharp interfaces. These alternating, ultrathin layers form a one-dimensional periodic structure, which is referred to as a superlattice. Among the most extensively studied superlattices is the one consisting of alternating layers of GaAs and  $\text{Al}_x\text{Ga}_{1-x}\text{As}$ .

In recent years there has been an increasing interest in the theoretical<sup>1-14</sup> and experimental<sup>15-21</sup> investigation of the behavior of shallow hydrogenic donor impurities in semiconductor heterostructures, quantum wells, and superlattices. In one of the early calculations<sup>1</sup> of the hydrogenic impurity states in  $\text{GaAs}/\text{Al}_x\text{Ga}_{1-x}\text{As}$  quantum wells (QW's), an infinite potential was assumed at the interfaces. Several groups<sup>2-5</sup> have extended the work of Bastard<sup>1</sup> to calculate the low-lying energy levels of a donor in the finite high barrier QW. Chaudhuri and Bajaj<sup>6</sup> included the effect of band nonparabolicity in their calculation where the effective mass of the electron was only associated with the lowest subband of the QW. The polaron effect of a quasi-two-dimensional electron gas interacting with longitudinal-optical (LO) phonons in the presence and absence of a magnetic field has been studied extensively<sup>22-31</sup>. Most of these works thus far have been concentrated on the resonant polaron effect of free electrons. Polaron correction to the properties of donors in a *single quantum well* was investigated by several groups<sup>7-11</sup>, where in Ref. 7 nonparabolic band mass was used for the lowest subband of the QW.

Chaudhuri<sup>12</sup> extended the variational calculation of the ground-state energy of a donor electron in a QW to the situation of a multiple-well structure. This calculation was generalized to a superlattice by Lane and Greene,<sup>13</sup> who also calculated the energy of low-lying excited states

( $2p^\pm$ ) of a hydrogenic donor at an arbitrary position. In Ref. 13 the effective mass of the electron was taken to be the bulk GaAs value throughout the whole superlattice. Recently Helm *et al.*<sup>32</sup> extended these calculations to higher excited states (i.e.,  $1s, 2s, 2p^\pm, 2p_z$ ), where they included the spatial dependence of the electron mass. All of the above calculations<sup>12,13,32</sup> are for zero magnetic field. In the present paper we will generalize them to nonzero magnetic field. At present we are unaware of any calculation of the donor states with LO-phonon interaction in a *superlattice* in the presence of a magnetic field. Polaron effects are present in polar semiconductors like GaAs. This effect results in a shift of the energies in low magnetic fields, and leads to a resonant splitting of the energies in high magnetic fields ( $B > 12$  T). Such effects have been observed in recent experiments.<sup>18-21</sup>

In this paper, we report on a calculation of the transition energies  $1s \rightarrow 2p^\pm$  for a shallow donor impurity associated with the lowest subband of a  $\text{GaAs}/\text{Al}_x\text{Ga}_{1-x}\text{As}$  superlattice in a magnetic field parallel to the growth axis. The position of the donor is arbitrary. We have included the mass discontinuity of the electron at the interface and the finite height of the barriers. To obtain the wave functions and energy levels of an electron in the absence of electron-phonon interaction, a variational approach is used in which the trial wave functions are Gaussians with two variational parameters and the effect of the nonparabolic band mass is included in a self-consistent manner. Polaron correction to these energies is calculated within second-order perturbation theory. We find that the polaron correction is important, not only at resonance, but also at lower magnetic fields, and that the effect of band nonparabolicity is appreciable in high magnetic fields. No interface phonons have to be invoked in order to explain the existing experimental data.<sup>15-21</sup> This paper is organized as follows. In Sec. II a variational calculation of the  $1s, 2p^\pm$  states is presented in the absence of the electron-phonon interaction. The polaron correction is calculated in Sec. III. A detailed

comparison with the experimental data is given in Sec. IV. Our discussions and conclusions are presented in Sec. V.

## II. VARIATIONAL APPROACH

Within the framework of an effective-mass approximation, the total Hamiltonian for a single conduction-band electron coupled to a Coulombic impurity and interacting with LO phonons is given by

$$H = H_e + H_{LO} + H_I, \quad (1)$$

where  $H_e$  is the electronic part

$$H_e = \frac{1}{2m_e^*(z)} \left[ \mathbf{p} + \frac{e}{c} \mathbf{A} \right]^2 - \frac{e^2}{\epsilon_0 r} + V_b(z), \quad (2)$$

which describes a hydrogenic atom placed in a superlattice in an external magnetic field, where the potential is modeled by a square-well potential

$$V_b(z) = \begin{cases} 0, & -w/2 + n(w+b) < z < w/2 + n(w+b) \\ V_0, & w/2n(w+b) < z < -w/2 \\ & + (n+1)(w+b), \end{cases} \quad (3)$$

with  $w$  the well width,  $b$  the barrier width, and  $n$  an integer. For a GaAs/Al<sub>x</sub>Ga<sub>1-x</sub>As interface the barrier height  $V_0$  is given by 60% of the total energy-band-gap difference between the two semiconductors:  $\Delta E_g = 1.155x + 0.37x^2$  eV.<sup>33</sup> The position of the electron is denoted by  $r = [\rho^2 + (z - z_I)^2]^{1/2}$ ,  $\rho = (x^2 + y^2)^{1/2}$  being the distance in the  $x$ - $y$  plane, and  $z_I$  the position of the donor. The quantity  $m_e^*(z)$  is the electron effective mass, which is different in the two semiconductors: for GaAs  $m_w/m_e = 0.067$ , and for Al<sub>x</sub>Ga<sub>1-x</sub>As  $m_b/m_e = 0.067 + 0.083x$ .  $\epsilon_0 = 12.5$  is the static dielectric constant of GaAs, which is assumed to be the same in both materials. We take  $x = 0.3$ , except when we compare with the experimental results of Ref. 17, where  $x = 0.25$ .

In Eq. (1)  $H_{LO}$  is the LO-phonon Hamiltonian which is given by

$$H_{LO} = \sum_{\mathbf{q}} \hbar\omega_{\mathbf{q}} (a_{\mathbf{q}}^\dagger a_{\mathbf{q}} + \frac{1}{2}), \quad (4)$$

where  $a_{\mathbf{q}}^\dagger$  ( $a_{\mathbf{q}}$ ) is the creation (annihilation) operator of a LO phonon with wave vector  $\mathbf{q}$  and energy  $\hbar\omega_{\mathbf{q}}$ . For GaAs we take  $\hbar\omega_{\mathbf{q}} = \hbar\omega_{LO} = 36.25$  meV.<sup>34</sup>

The electron-phonon interaction in Eq. (1) is given by

$$H_I = \sum_{\mathbf{q}} (V_{\mathbf{q}} a_{\mathbf{q}} e^{i\mathbf{q}\cdot\mathbf{r}} + V_{\mathbf{q}}^* a_{\mathbf{q}}^\dagger e^{-i\mathbf{q}\cdot\mathbf{r}}), \quad (5)$$

where  $|V_{\mathbf{q}}|^2 = 4\pi\alpha\sqrt{\hbar/2m_w\omega_{LO}(\hbar\omega_{LO}/q)^2/V}$ , with  $V$  the volume of the system,  $\alpha = e^2\sqrt{m_w/2\hbar\omega_{LO}(1/\epsilon_\infty - 1/\epsilon_0)}/\hbar$  the dimensionless coupling constant, and  $\epsilon_\infty$  the high-frequency dielectric constant of GaAs. In our calculation we take  $\alpha = 0.068$ , being the value in the GaAs wells, which is a good approximation because most of the weight of the electron wave function is located in the wells. Furthermore, we take only the interaction with three-dimensional bulk GaAs phonon modes and in

so doing we neglect the effect of the superlattice on the phonon modes.

The vector potential  $\mathbf{A}$  is defined as  $\mathbf{A} = \frac{1}{2}\mathbf{B} \times \mathbf{r}$ . The magnetic field  $\mathbf{B}$  is taken along the growth axis which we take to be the  $z$  axis. It is convenient to write our problem in the cylindrical coordinate system

$$H_e = -\frac{m_w}{m_e^*(z)} (\nabla^2 - \gamma L_z - \frac{1}{4}\gamma^2 \rho^2) - \frac{2}{r} + V_b(z), \quad (6)$$

where the effective Bohr radius in GaAs,  $a_0^* = \hbar^2\epsilon_0/m_w e^2 = 98.7$  Å, is taken as the unit of length, and the effective rydberg  $\mathcal{R}^* = e^2/2\epsilon_0 a_0^* = 5.83$  meV as the unit of energy. In Eq. (6)  $L_z = -i(\partial/\partial\phi)$  is the  $z$  component of the angular momentum operator (in units of  $\hbar$ ) and  $\gamma$  is a dimensionless measure of the magnetic field,  $\gamma = e\hbar B/2m_w c \mathcal{R}^* = 0.148B$  (T).

The Schrödinger equation with the Hamiltonian  $H_e$  cannot be solved exactly. A variational calculation of the  $1s$ ,  $2p^+$  and  $2p^-$  states will be given. Because the electron energies related to the superlattice potential are much larger than the Coulombic energies, we explicitly factor out the lowest-energy solution of the one-dimensional superlattice potential  $f(z)$ . Consequently we write the donor variational wave function of the  $i$  state as

$$\psi_i(\rho, z, \phi) = f(z) G_i(\rho, z - z_I, \phi), \quad (7)$$

where  $G_i(\rho, z - z_I, \phi)$  describes the internal states of the donor and  $f(z)$  is the superlattice wave function

$$f(z) = \begin{cases} \cos(k_1 z), & -w/2 < z < w/2 \\ b_1 e^{-k_2 z} + b_2 e^{-k_2 z}, & w/2 < z < w/2 + b, \end{cases} \quad (8a)$$

which is periodically repeated, and  $f(z) = f(z + nl)$ , where  $l = w + b$  is the length of the period. The parameters  $k_1$ ,  $k_2$ ,  $b_1$ , and  $b_2$  are determined by the matching conditions at the interfaces. It is assumed that both  $f(z)$  and  $[1/m_e^*(z)]\partial f/\partial z$  are continuous across the interfaces. We find

$$k_1 = \sqrt{2m_w E_z}/\hbar, \quad k_2 = \sqrt{2m_b(V_0 - E_z)}/\hbar,$$

$$b_1 = \frac{1}{2} e^{-k_2 w/2} \left[ \cos(k_1 w/2) - \frac{k_1 m_b}{k_2 m_w} \sin(k_1 w/2) \right]$$

and

$$b_2 = \frac{1}{2} e^{k_2 w/2} \left[ \cos(k_1 w/2) + \frac{k_1 m_b}{k_2 m_w} \sin(k_1 w/2) \right].$$

The energy momentum relation is determined by the transcendental equation

$$\cos(k_2 l) = \cos(k_1 w) \cosh(k_2 b)$$

$$- \frac{1}{2} \left[ \frac{k_1 m_b}{k_2 m_w} - \frac{k_2 m_w}{k_1 m_b} \right] \sin(k_1 w) \sinh(k_2 b).$$

(8b)

In Eq. (7) only the nonpropagating electron state, i.e., the

lowest state with  $k_z=0$ , is needed.

Since the Hamiltonian has cylindrical symmetry, the  $z$  component of the angular momentum is a good quantum number, and consequently the  $\phi$  dependence of the wave functions is of the form  $e^{im\phi}$ , where  $m$  is the usual azimuthal quantum number. The Coulombic part of the wave function  $G_i(\rho, z, \phi)$  in a magnetic field is taken as a product of Gaussians

$$G_i(\rho, z, \phi) = \rho^{|m|} e^{im\phi} e^{-\alpha_i \rho^2 - \beta_i z^2}, \quad (9)$$

where the term  $e^{-\beta_i z^2}$  corrects for taking only the  $k_z=0$  state in  $f(z)$ . In Ref. 3 a linear combination of Gaussians

$$\langle \psi_{1s} | \psi_{1s} \rangle = C_{1s}, \quad (11a)$$

$$\langle \psi_{2p^\pm} | \psi_{2p^\pm} \rangle = \frac{1}{2\alpha_{2p^\pm}} C_{2p^\pm}, \quad (11b)$$

$$\langle \psi_{1s} | H_e | \psi_{1s} \rangle = \pi m_w \int_{-w/2}^{w/2+b} dz \frac{f^2(z)}{m_e^*(z)} \sum_{n=-\infty}^{\infty} e^{-2\beta_{1s}(z-z_I+nl)^2} \left[ 1 + \left( \frac{\gamma}{4\alpha_{1s}} \right)^2 + A_{1s}^{(n)}(z) + B_{1s}^{(n)}(z) \right], \quad (11c)$$

$$\langle \psi_{2p^\pm} | H_e | \psi_{2p^\pm} \rangle = \frac{\pi m_w}{\alpha_{2p^\pm}} \int_{-w/2}^{w/2+b} dz \frac{f^2(z)}{m_e^*(z)} \sum_{n=-\infty}^{\infty} e^{-2\beta_{2p^\pm}(z-z_I+nl)^2} \left[ 1 + \left( \frac{\gamma}{4\alpha_{2p^\pm}} \right)^2 \mp \frac{\gamma}{4\alpha_{2p^\pm}} + \frac{1}{2} A_{2p^\pm}^{(n)}(z) + \frac{1}{2} B_{2p^\pm}^{(n)}(z) [ |z-z_I+nl| - 2\alpha_{2p^\pm}(z-z_I+nl)^2 ] \right], \quad (11d)$$

where we defined the normalization constants

$$C_i = \frac{\pi}{2\alpha_i} \int_{-w/2}^{w/2+b} dz f^2(z) \sum_{n=-\infty}^{\infty} e^{-2\beta_i(z-z_I+nl)^2}, \quad (11e)$$

and the functions

$$A_i^{(n)}(z) = \frac{1}{2\alpha_i} \left[ \frac{m_e^*(z)}{m_w} V_b(z) + 2\beta_i - 4\beta_i^2(z-z_I+nl)^2 + 4\beta_i(z-z_I+nl) \frac{1}{f(z)} \frac{df(z)}{dz} - \frac{1}{f(z)} \frac{d^2f(z)}{dz^2} \right], \quad (11f)$$

$$B_i^{(n)}(z) = -\frac{m_e^*(z)}{m_w} \left[ \frac{2\pi}{\alpha_i} \right]^{1/2} \operatorname{erfc}(\sqrt{2\alpha_i}|z-z_I+nl|) \times e^{2\alpha_i(z-z_I+nl)^2}, \quad (11g)$$

with  $\operatorname{erfc}(z)$  the complementary error function.

In Fig. 1 we present the donor energies of the  $1s$ ,  $2p^+$ , and  $2p^-$  states in a (100 Å)/(100 Å) GaAs superlattice (solid curves) as a function of the magnetic field and compare them with the equivalent energies in a 100-Å QW (dashed curves). The donors are placed at the center of the well. As a reference we give also in Fig. 1 the bottoms of the first two free-electron states, i.e.,  $E_{z,1} + \frac{1}{2}\hbar\omega_c$

is assumed for  $G_i$  where the parameters  $\alpha_i$  and  $\beta_i$  are taken from Huzinaga,<sup>35</sup> who performed a detailed study of the use of Gaussian basis functions for hydrogenic atom energy levels. For not too small magnetic fields the difference with our approach is small. In the present paper, we take  $\alpha_i$  and  $\beta_i$  as variational parameters which minimize the unperturbed energy of the  $i$  state

$$E_i^0 = \frac{\langle \psi_i | H_e | \psi_i \rangle}{\langle \psi_i | \psi_i \rangle}. \quad (10)$$

With the variational wave functions, Eqs. (7)–(9), we obtain the following expressions:

and  $E_{z,1} + \frac{3}{2}\hbar\omega_c$ , which are indicated by the dotted curves. Note that the binding energy of the donor states is given by  $\Delta E_i^0 = E_{z,1} + \frac{1}{2}\hbar\omega_c - E_i^0$  for  $i=1s, 2p^-$ , and  $\Delta E_{2p^+}^0 = E_{z,1} + \frac{3}{2}\hbar\omega_c - E_{2p^+}^0$ , where  $\omega_c = eB/m_w c$  is the

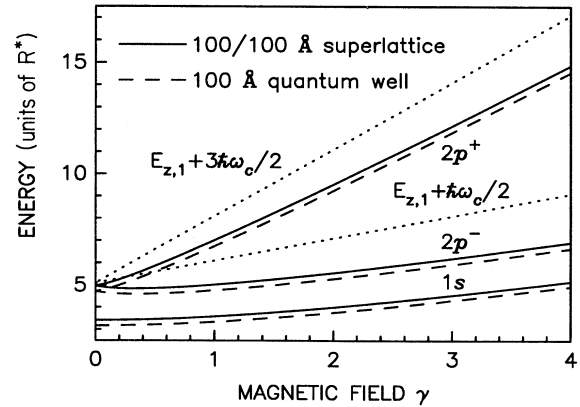


FIG. 1. Energy levels of a donor at the center of the well in units of the effective rydberg  $R^* = 5.83$  meV in a GaAs/Al<sub>0.3</sub>Ga<sub>0.7</sub>As, (100 Å)/(100 Å) superlattice (solid curves) and in a 100 Å QW (dashed curves) as a function of magnetic field  $\gamma = 0.148B$  (T). The two lowest Landau levels in the first subband are given by the dotted lines.

cyclotron resonance frequency for a noninteracting electron, and  $E_{z,1}$  is the energy of a free electron in the lowest subband at zero magnetic field. The energies for the two lowest subbands are  $E_{z,1}=5.10\mathcal{R}^*=29.74$  meV and  $E_{z,2}=19.94\mathcal{R}^*=116.25$  meV for the superlattice case,  $E_{z,1}=5.11\mathcal{R}^*=29.77$  meV and  $E_{z,2}=20.01\mathcal{R}^*=116.66$  meV for the QW case. Because of the large thickness of the barrier, the electron energies  $E_{z,1}$  and  $E_{z,2}$  corresponding to the superlattice are very close to those of the QW. In the superlattice the donor-electron wave functions are more spread out in comparison to the QW case, because the electron is able to leak into the adjacent wells, which diminishes the Coulombic energy  $\Delta E_i^0$  and consequently leads to larger energies  $E_i^0$  for the superlattice donor states as compared to the QW case.

The numerical results for the state widths of the well-center donors in the  $x$ - $y$  plane ( $\langle x^2+y^2 \rangle^{1/2}/\sqrt{2}$ ) and in the  $z$  direction ( $\langle (z-z_I)^2 \rangle^{1/2}$ ) are given in Fig. 2 as a function of the magnetic field in a  $(100 \text{ \AA})/(100 \text{ \AA})$  superlattice (solid curves) and in a  $100\text{-\AA}$  QW (dotted curves). Notice the following: (i) The results for the  $2p^+$  state are the same as those for the  $2p^-$  state, which is because the wave functions for both states, up to a phase factor, are the same. (ii) The  $1s$  state is more localized than the  $2p^\pm$  states, and the localization increases with increasing magnetic fields. The width of the wave function which is more spread out is more sensitive to the magnetic field. (iii) The wave functions are more localized in the  $z$  direction than in the  $x$ - $y$  plane because of the AlGaAs barriers. (iv) For a single quantum well of  $100 \text{ \AA}$  we found that the  $1s$  and  $2p^\pm$  states have the same width in the  $z$  direction, which is smaller than those for the superlattice case. The dependence of the width of the electron states on the position of the donor is depicted in Fig. 3 for a

magnetic field of  $\gamma=2.0$  (i.e.,  $B=13.5$  T). Notice that  $z_I=0, 50,$  and  $100 \text{ \AA}$  correspond to a donor at the center of the well, at the interface, and at the center of the barrier, respectively. For the QW case widths of the three states in the  $z$  direction share one curve. For the superlattice case the widths are a periodic function of the donor position as it should be, while for the QW case they are a monotonic increasing function of the distance from the center of the well. The width of the more localized state, i.e., the  $1s$  state, has a stronger dependence on the position of the donor than that of the more spread out states. A similar behavior is observed for the energy of these states (see Fig. 4).

The dependence of the energy levels of the  $1s$  and  $2p^+$  states on the donor position and the magnetic field is illustrated in Figs. 4(a) and 4(b) for the superlattice case ( $w=b=100 \text{ \AA}$ ) and in Figs. 4(c) and 4(d) for the QW case ( $w=100 \text{ \AA}$ ). We notice that (i) the energy of the  $1s$  state depends much more strongly on the position of the donor than that of the  $2p^+$  state; and (ii) once the donor is located inside the barrier, the difference between the superlattice and the QW cases is becoming appreciable.

### III. POLARON CORRECTION

Because GaAs is a weak polar material we can use second-order perturbation theory to calculate the polaron correction to the energy of the  $i$  state

$$\Delta E_i = - \sum_j \sum_q \frac{|\langle j; \mathbf{q} | H_I | i; \mathbf{0} \rangle|^2}{\hbar\omega_q + E_j^0 - E_i^0 - \Delta_i}, \quad (12)$$

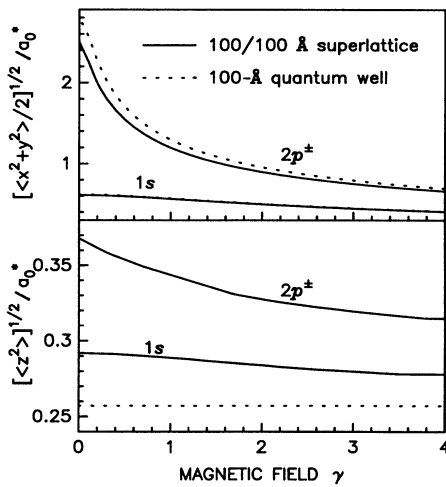


FIG. 2. Width of the well-center donor wave functions in the  $x$ - $y$  plane (upper figure), and in the  $z$  direction (lower figure) in units of the effective Bohr radius  $a_0^*=98.7 \text{ \AA}$  as a function of magnetic field in a  $(100 \text{ \AA})/(100 \text{ \AA})$  superlattice (solid curves) and in a  $100 \text{ \AA}$  QW (dotted curves).

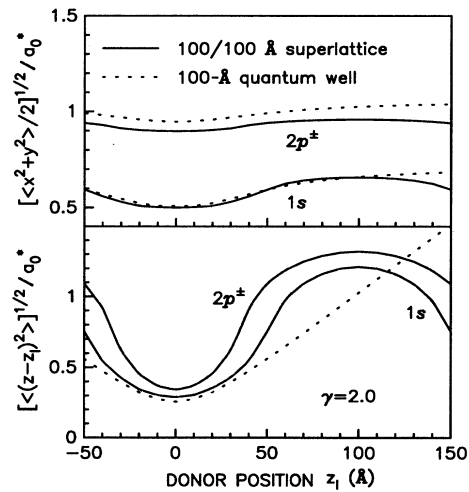


FIG. 3. Dependence of the width of the donor states in the  $x$ - $y$  plane (upper figure), in the  $z$  direction (lower figure) on the donor position in a superlattice ( $w=b=100 \text{ \AA}$ ) (solid curves), and in a QW ( $w=100 \text{ \AA}$ ) (dotted curves) in a magnetic field of  $\gamma=2.0$ .

where<sup>24,36,37</sup>  $\Delta_i = \Delta E_i - \Delta E_{1s}$ , and  $|j; \mathbf{q}\rangle$  describes a state composed by an electron with unperturbed energy  $E_j^0$  and a LO phonon with momentum  $\hbar\mathbf{q}$  and energy  $\hbar\omega_{\mathbf{q}}$ . In principle we have to include all donor states

in the sum  $\sum_j$ , which is a formidable task. In the present work we limit ourselves to the most important ones:  $1s$ ,  $2p^+$ , and  $2p^-$ . The matrix elements  $H_I^{i,j} = \sum_{\mathbf{q}} |\langle j; \mathbf{q} | H_I | i; \mathbf{0} \rangle|^2$ , in units of  $(\hbar\omega_{\text{LO}})^{3/2}$ , are given by

$$H_I^{1s,1s} = -\frac{\pi\alpha}{4\alpha_{1s}^2 C_{1s}^2} \int_0^\infty dq_z |G_{1s,1s}(q_z)|^2 \text{Ei} \left[ -\frac{q_z^2}{4\alpha_{1s}} \right] e^{q_z^2/4\alpha_{1s}}, \quad (12a)$$

$$H_I^{2p^\pm,1s} = H_I^{1s,2p^\pm} = \frac{\pi\alpha}{32\alpha_{1s}^2 \alpha_{2p^\pm} C_{1s} C_{2p^\pm}} \times \int_0^\infty dq_z |G_{1s,2p^\pm}(q_z)|^2 \left[ \frac{8\alpha_{1s}\alpha_{2p^\pm}}{\alpha_{1s} + \alpha_{2p^\pm}} + q_z^2 \text{Ei} \left[ -\frac{q_z^2(\alpha_{1s} + \alpha_{2p^\pm})}{8\alpha_{1s}\alpha_{2p^\pm}} \right] e^{q_z^2(\alpha_{1s} + \alpha_{2p^\pm})/8\alpha_{1s}\alpha_{2p^\pm}} \right], \quad (12b)$$

$$H_I^{2p^\pm,2p^\pm} = -\frac{\pi\alpha}{256\alpha_{2p^\pm}^4 C_{2p^\pm}^2} \times \int_0^\infty dq_z |G_{2p^\pm,2p^\pm}(q_z)|^2 \left[ 4\alpha_{2p^\pm}(12\alpha_{2p^\pm} + q_z^2) + (64\alpha_{2p^\pm}^2 + 16\alpha_{2p^\pm}q_z^2 + q_z^4) \text{Ei} \left[ -\frac{q_z^2}{4\alpha_{2p^\pm}} \right] e^{q_z^2/4\alpha_{2p^\pm}} \right], \quad (12c)$$

$$H_I^{2p^\pm,2p^\mp} = \frac{\pi\alpha}{256\alpha_{2p^\pm}^4 C_{2p^\pm}^2} \int_0^\infty dq_z |G_{2p^\pm,2p^\mp}(q_z)|^2 \left[ 16\alpha_{2p^\pm}^2 - 4\alpha_{2p^\pm}q_z^2 - q_z^4 \text{Ei} \left[ -\frac{q_z^2}{4\alpha_{2p^\pm}} \right] e^{q_z^2/4\alpha_{2p^\pm}} \right], \quad (12d)$$

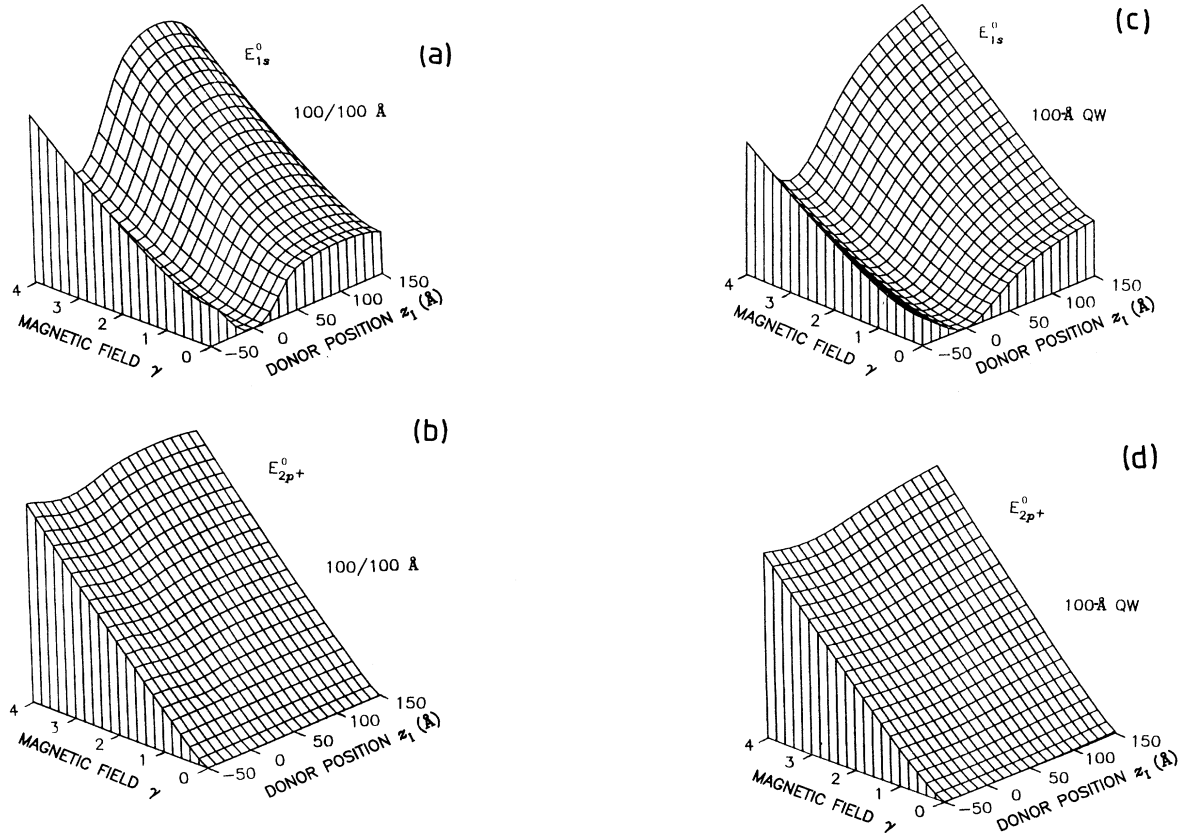


FIG. 4. Position and magnetic field dependence of the energies of a donor for (a) the ground state  $E_{1s}^0$  and (b) the excited state  $E_{2p^+}^0$  in a (100 Å)/(100 Å) superlattice and similarly in a 100 Å QW for (c)  $E_{1s}^0$  and (d)  $E_{2p^+}^0$ .

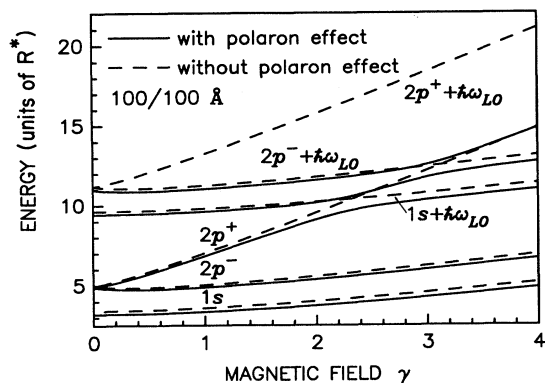


FIG. 5. Energy levels of a donor at the center of the well in a  $(100 \text{ \AA})/(100 \text{ \AA})$  superlattice as a function of the magnetic field with (solid curves) and without (dashed curves) electron-phonon interaction.

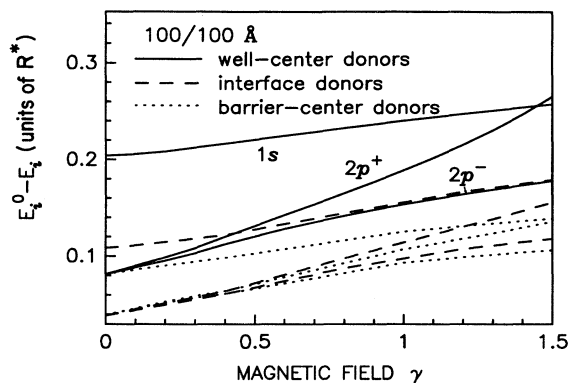


FIG. 6. Shift of the energy levels due to electron-phonon interaction vs the magnetic field for donors at the center of the well (solid curves), at the interface (dashed curves), and at the center of the barrier (dotted curves) of a superlattice ( $w = b = 100 \text{ \AA}$ ).

where we have defined the function

$$G_{i,j}(q_z) = \int_{-w/2}^{w/2+b} dz f^2(z) \sum_{n=-\infty}^{\infty} e^{-iq_z(z-z_I+nl) - (\beta_i + \beta_j)(z-z_I+nl)^2}, \quad (12e)$$

with  $\alpha_i, \beta_i$  the previously obtained variational parameters for the  $i$  state, and  $\text{Ei}(q_z)$  being the exponential integral function.

In Fig. 5 we depict the energy levels of the  $1s, 2p^\pm$  states (dashed curves) and the same ones shifted by a LO phonon for a donor at the center of the well of a GaAs/Al<sub>0.3</sub>Ga<sub>0.7</sub>As superlattice with  $w = b = 100 \text{ \AA}$ .

Note that (i) for not too large magnetic fields the polaron correction shifts the energy levels to lower energy, and these shifts increase with increasing magnetic field strength; and (ii) at resonance, i.e.,  $E_{2p^+}^0 = E_{1s}^0 + \hbar\omega_{LO}$  and  $E_{2p^-}^0 = E_{2p^+}^0 + \hbar\omega_{LO}$ , there are anticrossings of the energy levels.

The actual polaron shifts of the energy levels in low magnetic fields (i.e., below the resonance region) are shown in Fig. 6 for donors at the center of the well (solid curves), at the interface (dashed curves), and at the center of the barrier (dotted curves) of the  $(100 \text{ \AA})/(100 \text{ \AA})$  superlattice. In each of the three cases the  $1s$  state has the largest polaron correction and the  $2p^-$  state the smallest one. Furthermore, the polaron correction decreases when the donor moves away from the center of the well. Thus the smaller the width of the wave function of the donor state, the larger the polaron correction. The polaron correction to the  $2p^\pm$  states increase much more quickly with increasing magnetic field than that to the  $1s$  state because the width of the  $2p^\pm$  decreases much more quickly (see Fig. 2). The rapid increase of the polaron correction to the  $2p^+$  state for  $\gamma > 1$  is a result of the fact that this state is moving close to resonance.

#### IV. COMPARISON WITH EXPERIMENTS

In this section we compare our results with available experimental data. We first consider the system in relatively low magnetic fields, where there is no resonant polaron interaction and the electron-phonon interaction only induces a shift of the energies of the donor states. In Fig. 7(a) the experimental transition energies of Jarosik *et al.*<sup>15</sup> for donors at the center of the quantum well of a superlattice with  $w = 210 \text{ \AA}$  and  $b = 150 \text{ \AA}$  are plotted as a function of the magnetic field. We show our theoretical results with (solid curves) and without (dashed curves) electron-phonon interaction. Both the  $1s \rightarrow 2p^+$  and the  $1s \rightarrow 2p^-$  transition energies are in good agreement with the experimental data. For the case of narrower wells we show similar results in Fig. 7(b) for the experimental results of Cheng and McCombe<sup>16</sup> in a  $(125 \text{ \AA})/(125 \text{ \AA})$  superlattice. For broader wells such results are shown in Fig. 7(c) for the experimental data of Brozak and McCombe<sup>17</sup> in an  $x = 0.25, (450 \text{ \AA})/(125 \text{ \AA})$  superlattice. It is apparent from these figures that (i) the polaron effect slightly increases the transition energies, which is due to the fact (see Fig. 6) that the polaron correction to the  $1s$  state is larger than to the excited states  $2p^\pm$ , because the  $1s$  state is more localized; (ii) the polaron correction to these transition energies decreases with increasing magnetic field, which is a consequence of the fact that the polaron correction to the  $1s$  state increases less rapidly than the one to the  $2p^\pm$  states because the width of the wave function of the  $2p^\pm$  decreases more rapidly with increasing magnetic field than that of the  $1s$  state; and (iii) the

agreement is less satisfactory in the small magnetic-field region because we know<sup>32</sup> that at zero magnetic field the wave functions should be exponential rather than Gaussian.

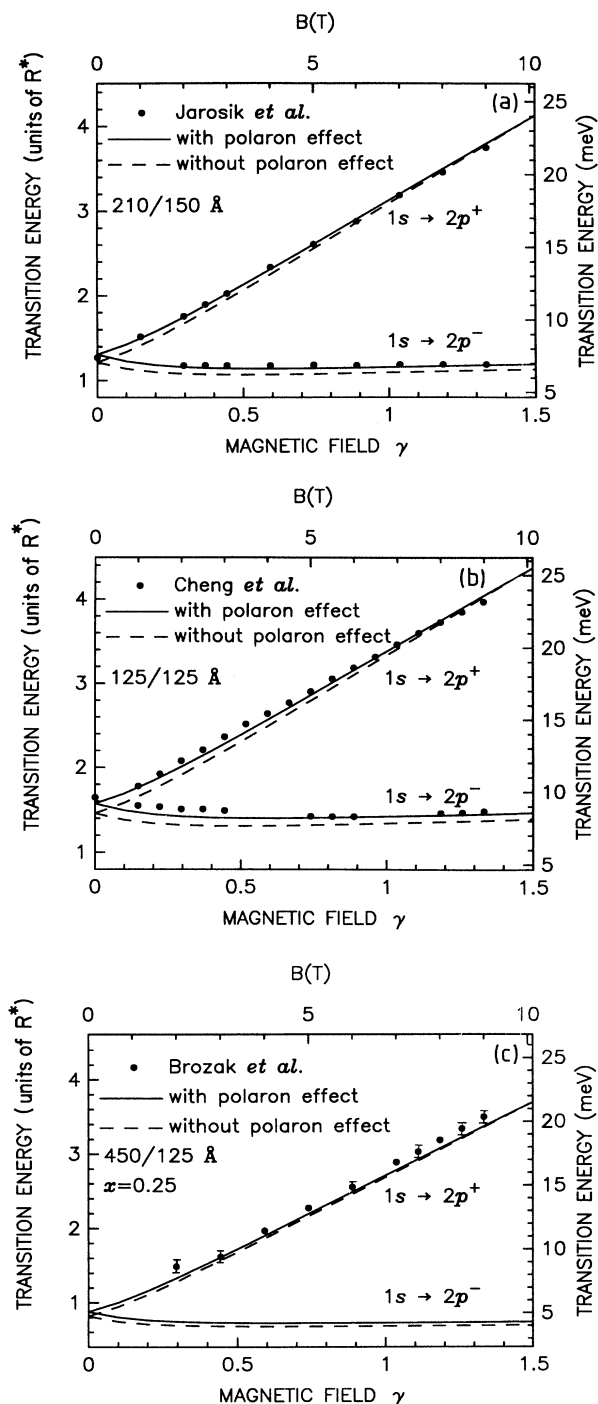


FIG. 7.  $1s \rightarrow 2p^{\pm}$  transition energies with (solid curves) and without (dashed curves) polaron corrections in  $x=0.3$  (a) (210 Å)/(150 Å), (b) (125 Å)/(125 Å), and (c)  $x=0.25$  (450 Å)/(125 Å) superlattices vs the magnetic field. The experimental data are from Jarosik *et al.* (Ref. 15), Cheng and McCombe (Ref. 16), and Brozak and McCombe (Ref. 17), respectively.

The  $1s \rightarrow 2p^+$  transition energy is shown in Fig. 8 as a function of the well width of the superlattice with a fixed barrier of width  $b=150$  Å in several low magnetic fields. Again we find good agreement with the experimental results of Jarosik *et al.*<sup>15</sup> if we include the polaron correction (solid curves). The polaron correction to  $E_{2p^+} - E_{1s}$  is more pronounced in lower magnetic fields and for narrower quantum wells.

For higher magnetic fields resonant polaron interaction can take place which alters the energy levels appreciably at resonance as was illustrated in Fig. 5. We compare in Fig. 9 the experimental results of Huan *et al.*<sup>18,19</sup> with the present theoretical calculation (dotted curves) for a superlattice with  $w=b=100$  Å in the cases of well-center donors, interface donors, and barrier-center donors. As a comparison we have also plotted the results for a single 100 Å QW (thin dashed curves). Notice that near resonance two transitions are observed which are a consequence of the lifting of the  $E_{2p^+}$  and  $E_{1s} + \hbar\omega_{LO}$  degeneracy. The experimental resonance positions, which in Refs. 18 and 19 were indicated, respectively, by the letters A, B, and C, are given in Fig. 9. Only for the well-center and interface donors we find good agreement with the experimental results in low magnetic fields. For  $\gamma > 1.5$  the agreement between theory and experiment is unsatisfactory. The reason is that for such high magnetic fields band nonparabolicity becomes important. We include this effect through an energy-dependent effective mass in the GaAs wells,

$$m_w(E)/m_e = 0.0665 + 0.0436E + 0.236E^2 - 0.147E^3, \quad (13)$$

where  $E$  is the single-electron energy of the  $i$  state in eV. The above expression is based on the  $\mathbf{k} \cdot \mathbf{p}$  approximation.<sup>38,39</sup> In order to obtain the unperturbed energy

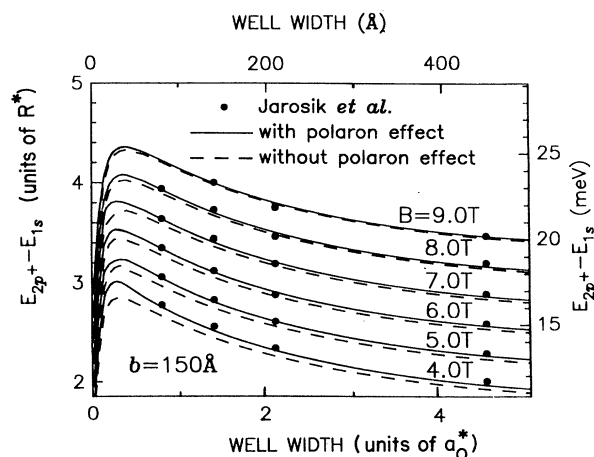


FIG. 8. Energy of the  $1s \rightarrow 2p^+$  transition in a GaAs/ $\text{Al}_{0.3}\text{Ga}_{0.7}\text{As}$  superlattice with a barrier width of 150 Å as a function of the well width for various magnetic fields with (solid curves) and without (dashed curves) polaron effects. The experimental data are from Jarosik *et al.* (Ref. 15).

$E = E_i^0$  and wave function  $\psi_i$  we have to solve Eq. (10) using Eq. (8b) for the lowest subband energy and Eq. (13) for the effective mass in a self-consistent manner. The results of such a calculation are given by the solid curves in Fig. 9. The agreement with the experimental results for the well-center and the barrier-center donors is excellent, while for the interface donors it is worse. A possible explanation for the latter discrepancy will be deferred to Sec. V.

Because the above self-consistent approach to include an energy-dependent mass is numerically very time consuming, it is interesting to consider different approximations which do not invoke this self-consistency. The simplest one would be to take  $E = E_{z,1}$  in Eq. (13). A first improvement to the latter approach is to consider  $E = E_{z,1} + \frac{1}{2}\hbar\omega_c$ , and a second improvement is to take  $E = E_{z,1} + \frac{1}{2}\hbar\omega_c$  for the  $1s$  and  $2p^-$  states, and

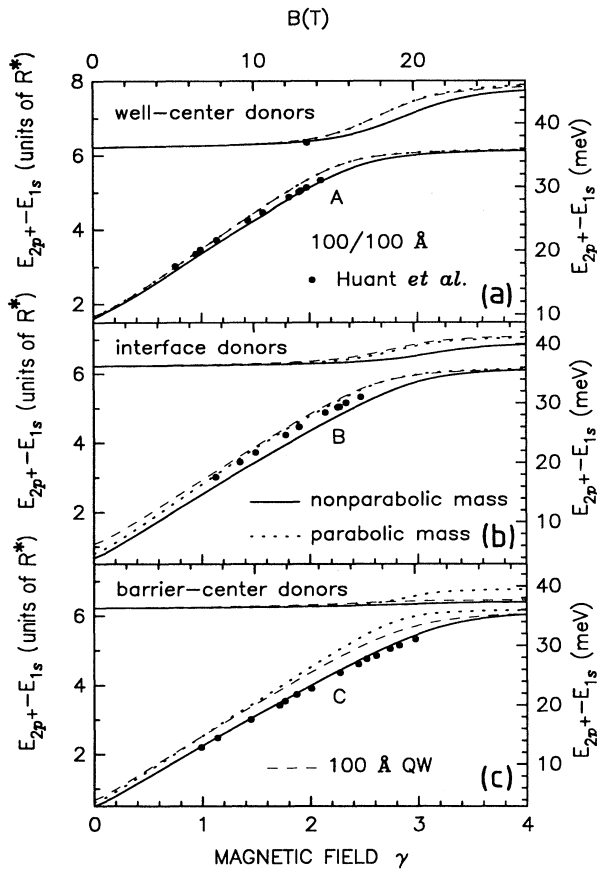


FIG. 9.  $1s \rightarrow 2p^+$  transition energies in a GaAs/ $\text{Al}_{0.3}\text{Ga}_{0.7}\text{As}$ , (100 Å)/(100 Å) superlattice as a function of magnetic field for donors at the center of the well (top figure), at the interface (middle figure), and at the center of the barrier (bottom figure). We compare our theoretical results for the cases of nonparabolic mass (solid curves), parabolic mass (dotted curves), and a 100 Å QW with parabolic mass (thin dashed curves) to the experimental data from Huant *et al.* (Refs. 18 and 19).

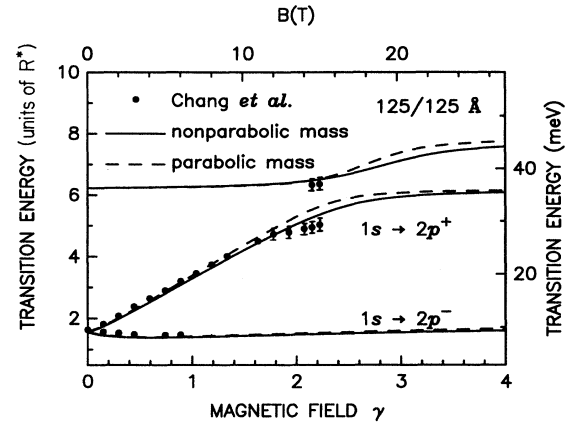


FIG. 10. Energies of the  $1s \rightarrow 2p^{\pm}$  transitions vs the magnetic field for donors at the center of the well in a (125 Å)/(125 Å) superlattice with (solid curves) and without (dashed curves) band nonparabolicity compared to the experimental data of Chang *et al.* (Ref. 20).

$E = E_{z,1} + \frac{3}{2}\hbar\omega_c$  for the  $2p^+$  state in Eq. (13). For a donor at the well center in a (100 Å)/(100 Å) superlattice in a magnetic field of  $\gamma = 2.0$  we found for the above approximations  $E_{2p^+} - E_{1s} = 5.35, 5.31, 5.29, 5.11, 5.13\mathcal{R}^*$ , respectively, where the first is for the parabolic mass and the last for the full self-consistent calculation. For a donor at the interface the results are  $E_{2p^+} - E_{1s} = 4.76, 4.55, 4.52, 4.32, 4.34\mathcal{R}^*$ , and for a barrier-center donor  $E_{2p^+} - E_{1s} = 4.52, 4.18, 4.14, 3.96, 3.99\mathcal{R}^*$ . Thus it is obvious that the second improvement is the best approximation, which can be reliably used to replace the full self-consistent calculation.

Recently Chang *et al.*<sup>20</sup> measured the transition ener-

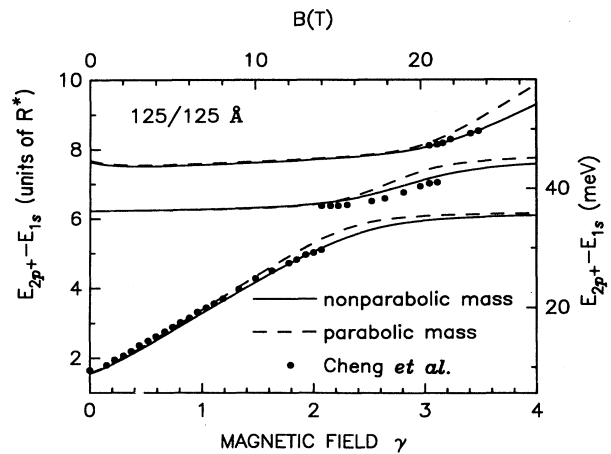


FIG. 11 Energy of the  $1s \rightarrow 2p^+$  transition for donors at the center of the well in a (125 Å)/(125 Å) GaAs-superlattice as a function of the magnetic field with (solid curves) and without (dashed curves) band nonparabolicity. The dots are the results of Cheng *et al.* (Ref. 21).

gies  $1s \rightarrow 2p^\pm$  for donors at the center of the well (solid dots in Fig. 10) for a GaAs/Al<sub>0.3</sub>Ga<sub>0.7</sub>As superlattice with well width  $w = 125 \text{ \AA}$  and barrier width  $b = 125 \text{ \AA}$ . Our present theoretical results with (solid curves) and without (dashed curves) band nonparabolicity are also given in Fig. 10. The overall agreement with the experiment is convincing. For very small magnetic fields the agreement is not as good because in that region the wave functions should be more exponential-like than Gaussian. For larger magnetic fields, i.e.,  $\gamma > 2.0$ , the experiment for the lower branch of the  $1s \rightarrow 2p^\pm$  transition shows a stronger polaron interaction than those found from our theoretical analysis. In Ref. 7 the interaction with interface phonons was invoked to explain this stronger phonon interaction.

Very recently Cheng *et al.*<sup>21</sup> were able to observe three branches in a (125 Å)/(125 Å) superlattice, whose results are depicted in Fig. 11 by solid dots. The results of the present calculation are given by the solid curves. Notice that the correction due to band nonparabolicity is essential to explain the experimental results, and no interaction with interface phonons has to be invoked.

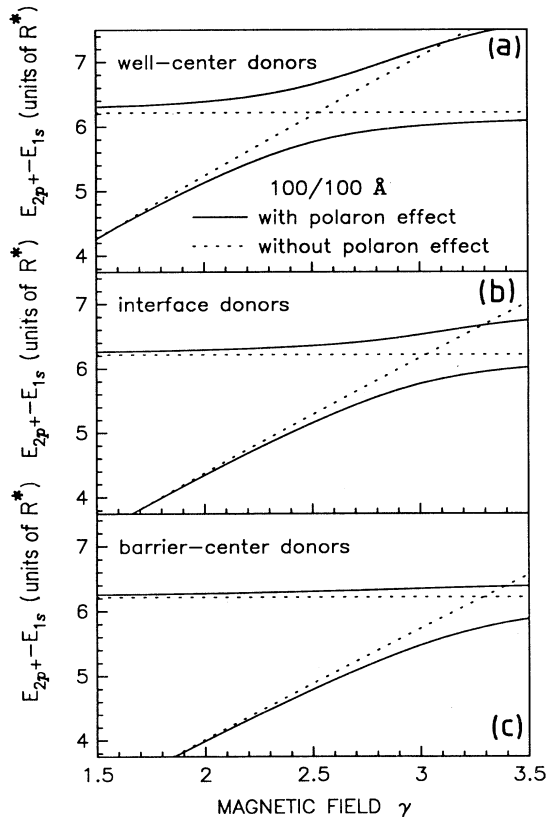


FIG. 12.  $1s \rightarrow 2p^\pm$  transition energy around resonance, with (solid curves) and without (dotted curves) polaron effect in a superlattice with  $w = b = 100 \text{ \AA}$  for donors at the center of the well (top figure), at the interface (middle figure), and at the center of the barrier (bottom figure) vs the magnetic field with band nonparabolicity.

## V. DISCUSSION AND CONCLUSION

We have investigated the  $1s \rightarrow 2p^\pm$  transition energies of shallow donor impurities in GaAs/Al<sub>x</sub>Ga<sub>1-x</sub>As superlattices in a magnetic field along the direction of the growth axis. The electron-LO-phonon-interaction-induced correction to these energies is included in our calculations. We find that the electron-phonon interaction increases the transition energies in low magnetic fields, and leads to resonant splitting of energies in high magnetic fields. We have considered the donors to be located at any position of the superlattice. In high magnetic fields, i.e.,  $\gamma > 1.5$ , the effect of band nonparabolicity is important. Our calculation, which contains *no* fitting parameters, is in good agreement with most of the available experimental data.

Recently Huan *et al.*<sup>18</sup> have argued that the resonant polaron interaction is larger for donors at the interface than those at the center of the well. In order to check this assertion we plot in Fig. 12 the transition energy, including band nonparabolicity, with (solid curves) and without (dotted curves) polaron correction near resonance for donors at the center of the well, at the interface and at the center of the barrier in a (100 Å)/(100 Å) superlattice. First notice that the resonant magnetic field increases with increasing distance of the donor from the center of the well. This implies that below resonance the polaron correction to the transition energies at a *fixed* magnetic field decreases with increasing distance of the donor from the center of the well because we are farther away from the polaron resonance field. At resonance let us denote the polaron energy shift by  $\Delta^-$  for the lower branch and by  $\Delta^+$  for the upper branch. The total splitting at resonance is thus given by  $\Delta = \Delta^- + \Delta^+$ . We found  $\Delta^- = 0.44, 0.43, 0.46 R^*$ ;  $\Delta^+ = 0.46, 0.33, 0.16 R^*$ ; and  $\Delta = 0.90, 0.76, 0.62 R^*$  for donors at the center of the well, at the interface, and at the center of the barrier, re-

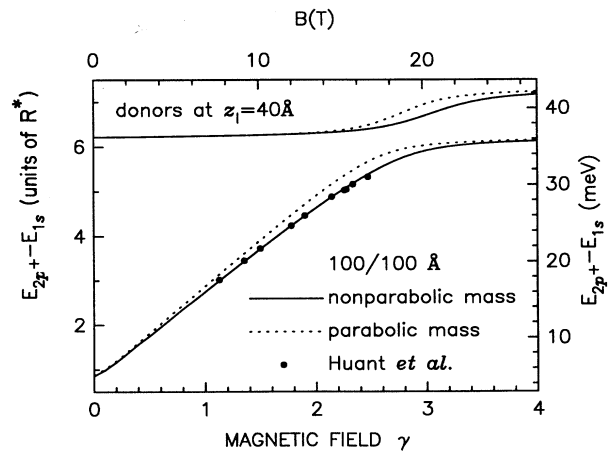


FIG. 13.  $1s \rightarrow 2p^\pm$  transition energy as a function of the magnetic field for donors at  $z_l = 40 \text{ \AA}$  in a (100 Å)/(100 Å) superlattice with (solid curves) and without (dotted curves) band nonparabolicity. The dots are the results of Huan *et al.* (Ref. 18).

spectively. Thus within the present approximation the well-center donors have the strongest polaron interaction.

In discussing the experimental results of Huant *et al.*<sup>18</sup> we confirmed that the resonance peak "B" could not be explained by transition energies from the interface donors (see Fig. 9). Recently<sup>40</sup> this B peak was interpreted as due to the negative-donor ( $D^-$ ) center  $\rightarrow n=1$  photoionization transition of a  $D^-$  center in the quantum well. This seems to agree with a recent theoretical calculation<sup>41</sup> of the binding energy of a  $D^-$  center in a single quantum well. In some of the early experimental samples,<sup>42,43</sup> however, an additional layer of donors was placed in the QW at 10 Å from the interface, i.e.,  $z_I=40$  Å, which motivated us to calculate the transition energies  $E_{2p^+} - E_{1s}$  corresponding to such donors. The results of such calculation are depicted in Fig. 13 and compared to the B transition. To our surprise excellent agreement with the experimental data is found. Nevertheless, we believe that this agreement is rather accidental because in most of the samples no such layer of donors was placed at 10 Å from the interface and the B peak was still observed.<sup>19</sup>

Finally, we would like to discuss the possibility of in-

creased polaron effects due to interaction with interface phonons. With the exception of Fig. 10 all experimental results discussed in the present paper could be explained by considering only interaction with three-dimensional bulk LO phonons. Recently we discussed in Ref. 44 the effect of interface phonons on the polaron ground-state energy and effective mass in the absence of a magnetic field. We found that for quantum wells of width  $w > 100$  Å such an effect was very small, which seems to corroborate our present analysis in nonzero magnetic fields. Therefore the results of Ref. 20 (see Fig. 10) for  $\gamma > 2.0$  are difficult to understand, and require further study.

#### ACKNOWLEDGMENTS

One of us (F.M.P.) is supported by the Belgian National Science Foundation. J.M.S. wishes to thank the International Culture Co-operation of Belgium for support. This work was supported by the Fonds voor Kollektief Fundamenteel Onderzoek (FKFO) Project No. 2.0093.91 and by IUAP-11. During the course of this work we have benefited from stimulating discussions with S. Huant, J. Singleton, C. Langerak, and B. D. McCombe.

\*Also at University of Antwerp, Rijksuniversitair Centrum te Antwerpen, Groenenborgerlaan 171, B-2020 Antwerpen, Belgium and Eindhoven University of Technology, NL-5600 MB Eindhoven, The Netherlands.

<sup>1</sup>G. Bastard, Phys. Rev. B **24**, 4714 (1981).

<sup>2</sup>C. Mailhoit, Y. C. Chang, and T. C. McGill, Phys. Rev. B **26**, 4449 (1982).

<sup>3</sup>R. L. Greene and K. K. Bajaj, Solid State Commun. **45**, 825 (1983); Phys. Rev. B **31**, 913 (1985); **37**, 4604 (1988).

<sup>4</sup>K. Jayakumar, S. Balasubramanian, and M. Tomak, Phys. Rev. B **34**, 8794 (1986).

<sup>5</sup>C. Priester, G. Bastard, G. Allan, and M. Lannoe, Phys. Rev. B **30**, 6029 (1984).

<sup>6</sup>S. Chaudhuri and K. K. Bajaj, Phys. Rev. B **29**, 1803 (1984).

<sup>7</sup>D. L. Lin, R. Chen, and T. F. George, Phys. Rev. B **43**, 9328 (1991).

<sup>8</sup>C. D. Hu and Y. H. Chang, Phys. Rev. B **40**, 3878 (1989).

<sup>9</sup>A. Erçelebi and M. Tomak, Solid State Commun. **54**, 883 (1985).

<sup>10</sup>B. A. Mason and S. D. Sarma, Phys. Rev. B **33**, 8379 (1986).

<sup>11</sup>F. A. P. Osório, M. Z. Maialle, and O. Hipólito, in *Proceedings of the 20th International Conference on the Physics of Semiconductors*, edited by E. M. Anastassakis and J. D. Joannopoulos (World Scientific, Singapore, 1990), p.1017.

<sup>12</sup>S. Chaudhuri, Phys. Rev. B **28**, 4480 (1983).

<sup>13</sup>P. Lane and R. L. Greene, Phys. Rev. B **33**, 5871 (1986).

<sup>14</sup>K. Tanaka, M. Nagaoka, and T. Yamabe, Phys. Rev. B **28**, 7068 (1983).

<sup>15</sup>N. C. Jarosik, B. D. McCombe, B. V. Shanabrook, J. Comas, J. Ralsto, and G. Wicks, Phys. Rev. Lett. **54**, 1283 (1985).

<sup>16</sup>J. P. Cheng and B. D. McCombe, Phys. Rev. B **42**, 7626 (1990).

<sup>17</sup>G. Brozak and B. D. McCombe, Phys. Rev. B **40**, 1265 (1989).

<sup>18</sup>S. Huant, W. Knap, G. Martinez, and B. Etienne, Europhys. Lett. **7**, 159 (1988).

<sup>19</sup>S. Huant, S. P. Nadja, W. Knap, G. Martinez, B. Etienne, C.

J. G. M. Langerak, J. Singleton, R. A. J. Thomeer, G. Hai, F. M. Peeters, and J. T. Devreese, in *Proceedings of the 20th International Conference on the Physics of Semiconductors* (Ref. 11), p. 1369.

<sup>20</sup>Y. H. Chang, B. D. McCombe, J. M. Mercy, and A. A. Reeder, Phys. Rev. Lett. **61**, 1408 (1988). A well width of  $w = 138$  Å was given here which should read  $w = 125$  Å; B. D. McCombe (private communication).

<sup>21</sup>J. P. Cheng, B. D. McCombe, G. Brozak, J. Ralston, and G. Wicks, Quantum Well and Superlattice Physics III [SPIE Proc. **1283**, 281 (1990)].

<sup>22</sup>S. D. Sarma and A. Madhukar, Phys. Rev. B **22**, 2823 (1980).

<sup>23</sup>R. Lassnig and W. Zawadzki, Surf. Sci. **142**, 388 (1984).

<sup>24</sup>F. M. Peeters and J. T. Devreese, Phys. Rev. B **31**, 3689 (1985).

<sup>25</sup>X. Wu, F. M. Peeters, and J. T. Devreese, Phys. Rev. B **34**, 8800 (1986).

<sup>26</sup>D. Larsen, Phys. Rev. B **40**, 4595 (1987).

<sup>27</sup>F. M. Peeters, X. Wu, and J. T. Devreese, Solid State Commun. **65**, 1505 (1988).

<sup>28</sup>X. Wu, F. M. Peeters and J. T. Devreese, Phys. Rev. B **40**, 4090 (1989).

<sup>29</sup>D. M. Larsen, Phys. Rev. B **30**, 4595 (1984).

<sup>30</sup>M. H. Degni and O. Hipólito, Phys. Rev. B **35**, 7717 (1987).

<sup>31</sup>M. H. Degani and O. Hipólito, Superlatt. Microstruct. **5**, 141 (1989).

<sup>32</sup>M. Helm, F. M. Peeters, F. Derosa, E. Colas, J. P. Harbison, and L. T. Florez, Phys. Rev. B **43**, 13983 (1991).

<sup>33</sup>H. J. Lee, L. Y. Juravel, J. C. Wolley, and A. J. SpringThorpe, Phys. Rev. B **21**, 659 (1980).

<sup>34</sup>S. Adachi, J. Appl. Phys. **58**, R1 (1985).

<sup>35</sup>S. Huzinaga, J. Chem. Phys. **42**, 1293 (1985).

<sup>36</sup>J. T. Devreese and F. M. Peeters, Solid State Commun. **58**, 861 (1986).

<sup>37</sup>G. Lindemann, R. Lassnig, W. Seidenbusch, and E. Gornik, Phys. Rev. B **28**, 4693 (1983).

- <sup>38</sup>R. M. Kolbas, Ph.D. thesis, University of Illinois at Urbana-Champaign, 1979 (unpublished).
- <sup>39</sup>U. Ekenberg, Phys. Rev. B **36**, 6152 (1987).
- <sup>40</sup>S. Huant, S. P. Najda, and B. Etienne, Phys. Rev. Lett. **65**, 1486 (1990).
- <sup>41</sup>T. Pang and S. G. Louie, Phys. Rev. Lett. **65**, 1635 (1990).
- <sup>42</sup>S. Huant, W. Knap, R. Stepniewski, G. Martinez, V. Thierry-Mieg, and B. Etienne, in *High Magnetic Fields in Semicon-*
- ductor Physics II*, edited by G. Landwehr, Springer Series in Solid State Science Vol. 87 (Springer-Verlag, Berlin, 1989), p. 293.
- <sup>43</sup>S. Huant, R. Stepniewski, G. Martinez, V. Thierry-Mieg, and B. Etienne, Superlatt. Microstruct. **5**, 331 (1989).
- <sup>44</sup>G. Q. Hai, F. M. Peeters, and J. T. Devreese, Phys. Rev. B **42**, 11 063 (1990).